6-DoF Robotic 3D Printing of Martian Habitat Components: Scaled Fabrication Model-Based Experimental Validation

Emrullah Koca[1] and Ahmet Türer[1]

[1]Middle East Technical University, Türkiye

kocaemrullah90@gmail.com, aturer@metu.edu.tr

Abstract

This study presents a 3D-printing workflow for Martian habitat components using a six-degree-of-freedom (6-DoF) robotic arm, experimentally validated through scaled fabrication models for future extraterrestrial construction. The printing system was developed at METU ROMER and integrates a custom hot-melt extrusion head with a Python - Robot Operating System (ROS) control interface. Toolpaths are generated using a Microsoft Excel-based coordinate generator that specifies X-Y-Z positions, wrist orientations, and motion speeds, enabling continuous deposition along complex trajectories. Calibration experiments were conducted to adjust printing parameters and evaluate controllability. Following calibration, demonstrations were performed using the Scaled Fabrication Model (SFM) approach: a 1/30-scale flat unit and a 1/35-scale Marsphere prototype were printed to verify multi-curved surface fabrication and uninterrupted toolpaths. In addition, a 1/30-scale cantilever box cross-section slab was printed to assess the feasibility of horizontal elements without formwork. Numerical analysis in SAP2000 predicted a maximum deflection of 0.4578 mm under dead load, and the printed slab exhibited close agreement with the measured free-end (tip) deflection, with the best-performing case matching the numerical prediction within approximately 1%. Overall, the results indicate that the proposed robotic workflow can fabricate key components relevant to future extraterrestrial construction, contributing an integrated Excel-to-ROS path-generation pipeline, a calibration-driven parameter window for repeatable deposition, and an experimental-numerical SFM validation strategy.

Keywords: Mars, 3D printing, 6-DoF robotic arm, Marsphere, slab printing, Mars habitation

1 Introduction

The construction of extraterrestrial habitats is a multidisciplinary challenge spanning structural engineering, materials science, robotics, and space architecture. On Mars, stringent environmental and logistical constraints make many terrestrial construction practices impractical. Limited payload capacity, reduced gravitational acceleration, extreme temperature fluctuations, and a thin atmosphere motivate construction systems that are material-efficient. These constraints have accelerated interest in additive manufacturing approaches that can fabricate structural components in situ [1, 2].

Within this context, robotic additive manufacturing has emerged as a promising alternative to traditional gantry-based 3D-printing systems. While gantry printers offer scalability, their constrained kinematics limit the fabrication of highly curved, multi-directional, or non-planar elements that are fundamental to pressure-containing and resilient extraterrestrial structures. By contrast, six-degree-of-freedom (6-DoF) robotic arms provide greater kinematic freedom, enabling multi-angled deposition, continuous toolpath execution, and the construction of complex forms without auxiliary formwork. However, this added flexibility typically increases the demands on calibration, collision-aware path planning, and process tuning, and the effective build envelope may be more constrained than large gantry systems. Recent studies, such as the work in [3] on 3D lattice structures and the Scaled Fabrication Model (SFM) framework proposed in [4], highlight the value of robotic systems for experimental validation when geometric precision and multi-axis deposition are critical. However, these studies often focus on either robotic fabrication of specific geometries or conceptual frameworks for scaled prototyping, without integrating the full sequence from coordinate generation and robotic control to application-level validation of habitat-relevant structural components. This gap is particularly important for Martian construction, where both multi-curved pressure-resisting shells and horizontal slab-type elements are essential to the architectural and structural system.

The SFM methodology fabricates scaled physical models using the same construction logic intended for full-scale deployment, thereby reducing uncertainty in constructability and process feasibility. In this paper, SFM is combined with a 6-DoF robotic platform to validate a robotic printing workflow for key architectural and structural components of a proposed Martian habitat, including multi-curved shell segments and a formwork-free slab element.

In this study, we develop and validate a robotic fabrication workflow for scaled production of Martian habitat components using a 6-DoF robotic arm and a custom extrusion system. Toolpaths are generated via an Excel-based coordinate generator to control position, orientation, and deposition speed. The workflow is evaluated through calibration and application-level demonstrations, including multi-curved shell segments (Marsphere) and a formwork-free cantilever slab, supported by comparison with numerical predictions.

The novelty of this study lies in the experimental validation of an integrated 6-DoF robotic printing workflow for Martian habitat components. Unlike previous studies that mainly emphasize isolated geometric printing or conventional gantry-based approaches, this work combines: (i) an Excel-based coordinate generation system for defining position, orientation, and motion speed; (ii) a Python-ROS interface for robotic execution; (iii) multi-curved shell printing within the Scaled Fabrication Model (SFM) framework; and (iv) formwork-free cantilever slab printing supported by comparison with SAP2000 predictions.

Accordingly, the main contributions of the study are: (1) development of a coordinate-driven Excel-to-ROS robotic fabrication pipeline; (2) experimental verification of continuous 6-DoF deposition along curved trajectories; (3) demonstration of a scaled Marsphere prototype as a constructability check for multi-curved habitat shells; and (4) validation of a formwork-free slab concept through experimental-numerical agreement in tip deflection.

2 Methodology

This study develops a robotic fabrication workflow using a UR5e 6-DoF robotic arm equipped with a custom hot-melt extrusion head and a Python- Robot Operating System (ROS) control interface [5]. To generate continuous deposition trajectories, a Microsoft Excel-based coordinate generator converts the digital geometry into robot commands, including X-Y-Z positions, end-effector orientations, and motion speeds.

The experimental program is structured in two stages: (i) calibration trials to identify a stable process window linking arm velocity and extrusion rate to bead geometry, and (ii) demonstration prints based on the SFM approach. These demonstrations include multi-curved shell segments and a formwork-free horizontal element to assess the geometric and structural feasibility of the workflow at scale.

2.1 Robotic Printing Setup

All additive manufacturing experiments were conducted at Middle East Technical University (METU) Robotics and Artificial Intelligence Technologies Research Center (ROMER) using a Universal Robots UR5e six-degree-of-freedom (6-DoF) robotic arm. The UR5e [6] provides a maximum reach of 850 mm and a compact footprint (Ø149 mm), enabling precise multi-axis manipulation within the available workspace.

A hot glue gun was mounted to the robot tool flange and used as the end-effector for material extrusion. To ensure continuous feeding of the hot-melt adhesive through the guide, a V-groove ball bearing driven by a 12 V DC motor was integrated into the feeding mechanism, providing stable transport and consistent deposition during printing. A cooling fan was positioned near the hot glue gun to accelerate solidification of deposited layers. This system provided controlled thermal conditions and stable mechanical feeding, improving deposition consistency.

Commercial hot glue sticks are typically 30 cm long; therefore, a continuous hot glue stick (100 m in length, 11 mm in diameter) was specially produced by Somafix to support uninterrupted printing trials. The overall setup is shown in Figure 1.

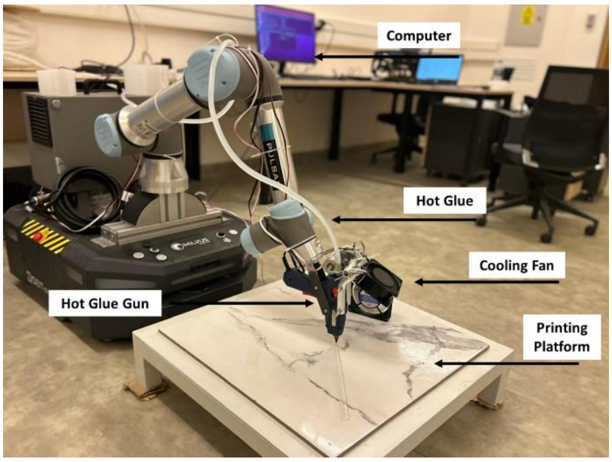

Figure 1. Setup of the 3D printing system

2.2 Coordinate Generation and Toolpath Planning

Effective coordination between the control software and the robotic hardware is essential for successful fabrication, particularly to synchronize robotic motion with extrusion behavior. Toolpaths were defined in a Microsoft Excel file and read by a PC running Python as the main controller. The Excel-based coordinate generator produces a waypoint table that represents the intended deposition trajectory and can be directly modified to adjust printing strategy for different geometries.

Each toolpath entry specifies workspace parameters including X-Y-Z coordinates, wrist orientation angles (RX, RY, RZ), and motion speed. Including wrist orientations allows the nozzle direction to be controlled along the path, which is required for continuous deposition on multi-curved surfaces and during transitions. The prescribed speed provides direct control over robot motion during printing and is used to regulate deposition behavior in combination with the extrusion system.

The exported dataset was processed using a Python-ROS control script, which converts the tabulated toolpath information into robot motion commands. ROS also provides the communication interface between the PC and the robotic arm, enabling synchronized execution of multi-axis movements during printing.

This coordinate-driven planning approach supports continuous deposition along complex trajectories, such as spherical surfaces, multi-curved transitions, and cantilever slab profiles, with a level of multi-axis control that is difficult to achieve using conventional gantry-based printing systems.

2.3 Material and Extrusion System

Hot-melt adhesive (hot glue), a thermoplastic material, was used as the printing material in all experiments. It was selected because it solidifies rapidly after extrusion, which supports stable layer-by-layer fabrication during scaled experimental validation of additive construction processes. This selection also enables controlled laboratory testing of robotic deposition behavior (e.g., continuity, adhesion, and layer formation) before full-scale material deployment is considered.

Material delivery was regulated using a DC motor integrated into the extrusion/feeding mechanism. By adjusting the motor actuation level, the extrusion rate could be adjusted to achieve consistent deposition and to reduce discontinuities during printing. In the experiments, the DC motor was operated using discrete voltage levels (3 V, 4.5 V, 6 V, 7.5 V, 9 V, and 12 V), which provided practical control points for calibrating material flow under different printing conditions.

To calibrate the process, preliminary linear-motion tests were conducted to quantify the relationship between robotic-arm travel speed, extrusion actuation level (voltage), and the resulting deposited bead geometry. These tests established the feasible operating window and were used to identify parameter combinations that produce stable and repeatable deposition. The test outcomes showed that layer width and height typically ranged from 2 to 8 mm depending on the selected motion speed and extrusion setting. The resulting observations were then used to guide parameter selection for the subsequent calibration prints and application-level demonstrations, helping maintain deposition uniformity and geometric fidelity across the printed components.

In this respect, the methodology is not limited to a material deposition setup alone; it establishes an integrated robotic fabrication workflow that links geometry definition, coordinate generation, multi-axis control, calibration, and application-level validation for Martian habitat components.

3 Experimental Validation and Results

3.1 Calibration Experiments

Prior to fabricating the scaled habitat components, calibration prints were carried out to evaluate system controllability and to refine printing parameters. Two representative geometries were selected: (i) a cylinder to assess layer consistency under predominantly planar motion, and (ii) a sliced spherical segment to evaluate multi-curved deposition and nozzle-orientation control.

Cylindrical specimen: A cylinder with a diameter of 15 cm and a height of 10 cm was printed using a nominal layer height of 2.5 mm and a motion speed of 5.5 mm/s. In the first trial, the print quality did not meet the expected standard: the deposited layers exhibited inconsistent alignment and adhesion, resulting in an uneven surface shown in Figure 2.

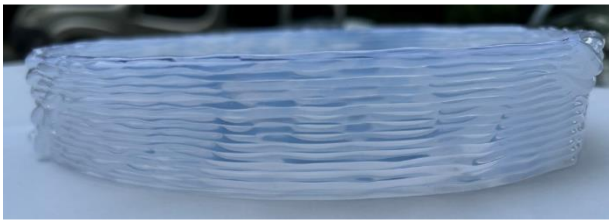

Figure 2. Cylinder shape at first trial

The uneven printing was caused by i) insufficient process synchronization in the code, i.e. uneven nozzle movement speed and overall speed, ii) layer height, iii) printing platform levelling, and iv) extrusion discharge speed. Irregularities not only change stress distribution but also may lead to weak interlayer bonding strength. Poor surface quality was another issue. After refining the printing parameters (layer height, extrusion conditions, and motion speed), a second cylinder print achieved improved surface finish and uniform layer adhesion (Figure 3).

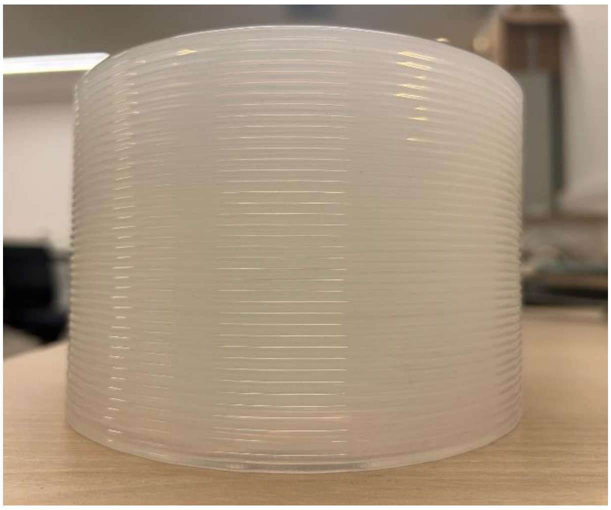

Figure 3. Targeted cylinder shape

- **Sliced spherical segment:** Sliced spherical segment with a diameter of 20 cm and a height of 15 cm was printed using a toolpath derived from the digital sphere model. The printed segment closely followed the programmed trajectory and showed stable layer formation along the curved path (Figure 4), demonstrating that the 6-DoF robotic arm can maintain both nozzle orientation and trajectory control during multi-curved deposition without interrupting the toolpath.

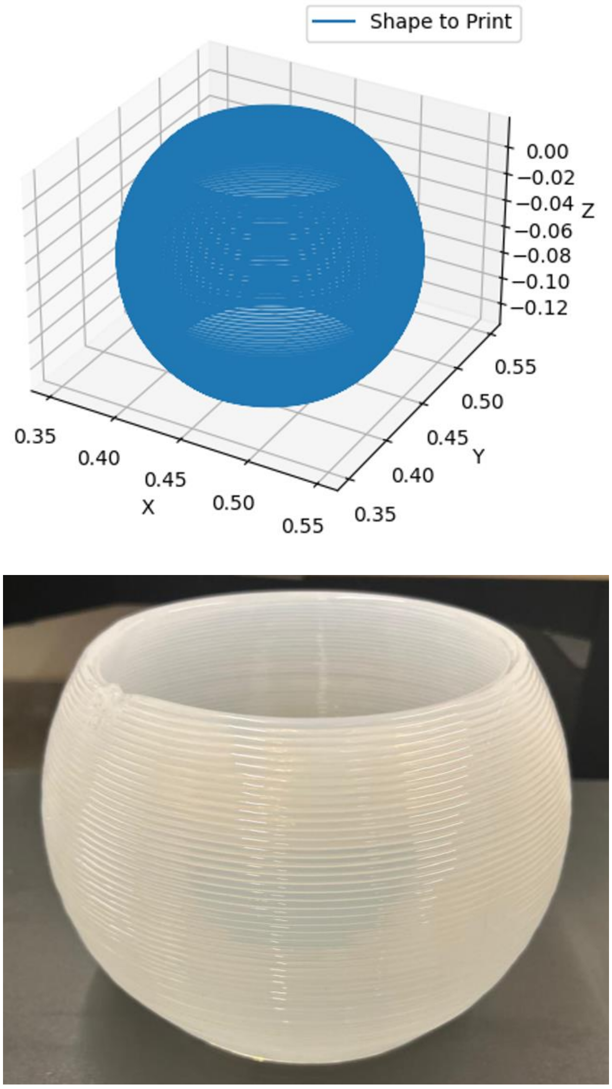

Figure 4. Sliced spherical segment

Overall, the calibration experiments clarified the interaction between robot motion parameters and deposition behavior. The cylinder trials indicated that stable layer adhesion requires appropriate synchronization between robot velocity, layer height, and extrusion conditions, while the sliced spherical segment demonstrated that the 6-DoF robotic arm can maintain nozzle orientation and trajectory control during multi-curved deposition without interrupting the toolpath. These observations were used to define a reliable parameter range for the subsequent application-level demonstrations. In these experiments, hot-melt adhesive (hot glue) is used as a process surrogate to evaluate deposition continuity and geometric fidelity, rather than to represent the mechanical performance of the target structural material. The scaled-down versions differ from the actual full-scale elements in terms of surface roughness and interlayer bond strength. 3D printing using

6 dof robotic arm ended up using accurate coordinates and the melted hot glue moulded over the shape of the previous layer's surface by following the lead of the printing nozzle. The dimensional accuracy was submillimetre and accepted as 100% correct. The surface roughness was also at submillimetre level, maximum indentation approximately measured as 0.3 mm. Actual wall thickness, nozzle shape, layer thickness will also differ from the lab specimen.

3.2 Application-Level Demonstrations

Following calibration, the workflow was applied to print scaled architectural and structural components relevant to the proposed Martian habitat concept, to assess geometric fidelity and constructability.

3.2.1 Flat Unit

A flat unit representing a residential layout was printed at a 1/30 prototype scale. The corresponding full-scale unit has plan dimensions of 9 m × 8 m (72 m²) and a floor height of 2.5 m. The digital model (Figure 5) illustrates the interior arrangement, and the 3D-printed scaled model reproduces key architectural elements, including interior partitions, window openings, and door locations. This printed unit serves as a physical reference for evaluating spatial configuration, proportions, and the geometric consistency of the proposed robotic printing workflow at reduced scale.

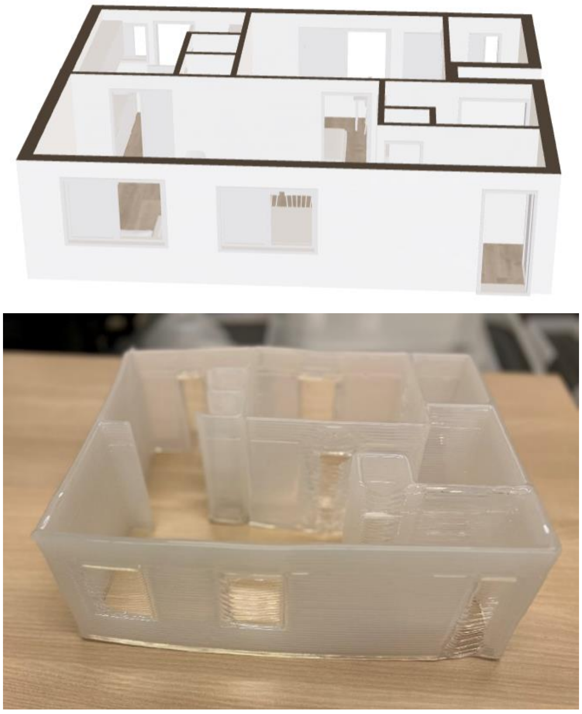

Figure 5. 3D printed scaled Flat model

3.2.2 Marsphere prototype

After successfully printing the cylinder, sliced sphere, and flat model, the calibration and printing process was confirmed to be controlled and accurate. Subsequently, the proposed Marsphere for Mars was 3D printed at a prototype scale of 1/35 (Figure 6). Rather than serving as an additional calibration print, this prototype functions as an application-level demonstration of continuous deposition on a free-form shell surface.

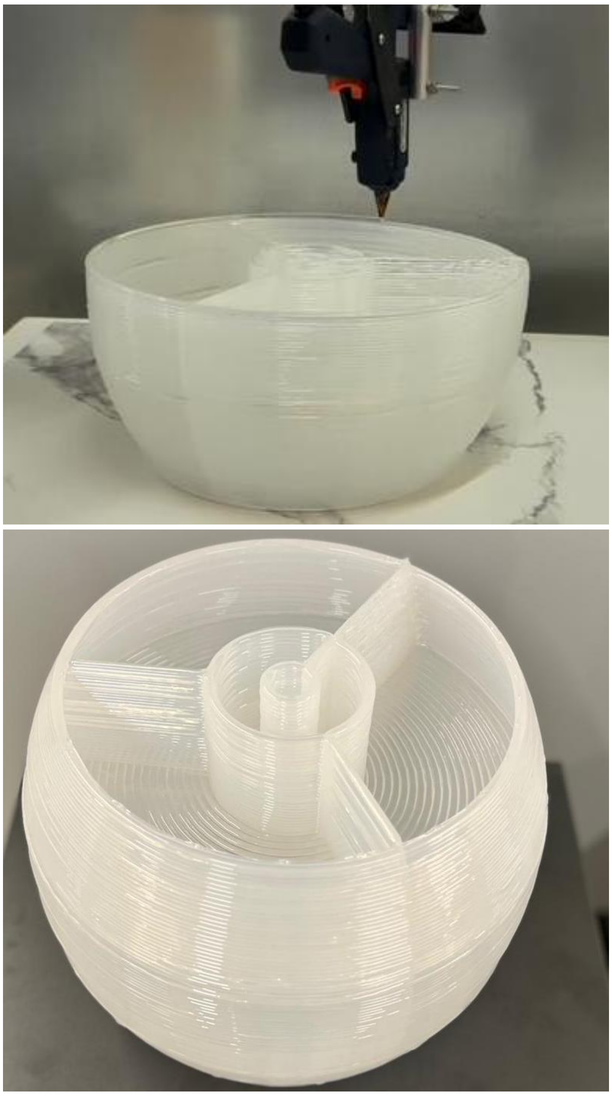

Figure 6. 3D Printed Scaled Model of the Marsphere

To frame this demonstration, the prototype is interpreted using the SFM concept introduced by [4], where a scaled physical model is fabricated using construction logic consistent with full-scale implementation. In this study, the printed Marsphere prototype provides physical feedback on toolpath continuity, curvature transitions, and layer formation, capabilities that are difficult to evaluate using digital simulation alone-and supports early design decision-making before full-scale trials.

3.2.3 Formwork-free cantilever slab

Although 3D printing has been widely explored for complex structural forms, such as the lattice structures investigated in [3], formwork-free printing of horizontal slab elements remains limited, primarily because gravity can cause deformation and loss of geometric stability during overhanging deposition.

To address this challenge within the Marsphere concept, this study focuses on printing an individual slab element to evaluate both printability and structural performance at scale.

For construction on Mars, a slab geometry with an optimized box cross-section was proposed for the Marsphere. A horizontal cantilever slab extending from a wall face was printed as a 1/30-scale prototype, with a width of 30 cm and a cantilever length of 13.5 cm. The box cross-section dimensions were 2 cm (width) × 1.67 cm (height), as shown in Figure 7.

Figure 7. 3D printed cantilever slab

To evaluate the expected response under self-weight, a SAP2000 numerical model of the prototype slab was developed and analyzed under dead load. The analysis predicted a maximum deflection of 0.4578 mm (Figure 8). The experimentally measured free-end (tip) deflection of the printed slab showed close agreement with the numerical prediction within ~1%, supporting the reliability of the simulation and demonstrating that the proposed robotic workflow can produce a stable, formwork-free horizontal element at the tested scale.

Figure 8. Maximum deflection of the Slab

These experiments collectively verified the precision, repeatability, and applicability of the developed robotic workflow for constructing key components of the proposed Martian habitat.

Therefore, the slab experiment should be understood not merely as a print demonstration, but as a novelty of the study in itself: it experimentally tests a horizontal structural component that is directly relevant to multi-storey Martian habitat construction and is rarely addressed in robotic construction printing studies.

3.3 Overall System Performance

Across all experiments, the robotic printing system demonstrated consistent extrusion behavior, uninterrupted toolpath execution, and repeatable fabrication outcomes. The successful printing of geometries spanning cylindrical and spherical calibration specimens, as well as architectural (flat unit) and structural (cantilever slab) components, indicates that the developed workflow can accommodate both planar and multi-curved deposition paths relevant to extraterrestrial habitat construction. Collectively, these results support the use of scaled robotic fabrication as a practical intermediary step between digital modelling and future full-scale programmed construction scenarios.

The calibration stage-consisting of the cylindrical specimen followed by the sliced spherical segment (20 cm diameter, 15 cm height)-verified reliable layer adhesion, controlled curvature formation, and stable nozzle orientation, establishing the parameter baseline used in the subsequent application-level demonstrations.

Beyond reporting successful print outcomes, these results demonstrate that the proposed workflow extends current robotic construction studies by validating not only geometric deposition, but also the coordinated interaction between path planning, nozzle orientation, and structural application. This is particularly significant for Martian habitat construction, where fabrication must address both free-form shell geometries and slab-like horizontal components within a unified construction logic.

4 Discussion

The experiments demonstrate that a 6-DoF robotic arm can execute continuous deposition along both simple and multi-curved trajectories when tool motion and extrusion are properly synchronized. The contrast between the initial and improved cylinder prints highlights the sensitivity of layer adhesion and surface regularity to the coupled effects of travel speed, extrusion rate, and cooling conditions. This emphasizes that parameter tuning is not a peripheral step but a primary determinant of print stability for thermoplastic-based deposition workflows. In other words, the experiments define a practical process window (motion-extrusion-cooling envelope) that governs geometric fidelity and repeatability. In this respect, the robotics-based 3D printing approach investigated here differs significantly from most Earth-based construction printing studies, which generally rely on cementitious materials that are weak in tension. In the present study, hot glue (silicone) is used only as a demonstration material and process replacement, while the ultimate target material for Mars is polyethylene, envisioned to be produced from Martian atmospheric CO_2 and water (H_2O).

Compared with prior studies in construction-oriented additive manufacturing, the present study contributes at a different level. Many existing investigations concentrate on gantry-based systems, vertical wall printing, or isolated geometric demonstrations. By contrast, this work validates a multi-axis robotic workflow that combines toolpath generation, nozzle-orientation control, curved shell fabrication, and formwork-free slab production within the same experimental framework. This distinction is important because Martian habitat construction cannot rely solely on wall-type extrusion logic; it requires coordinated fabrication of pressure-resisting shell geometries together with functional horizontal elements.

The Marsphere prototype provides a practical constructability check within the SFM logic: the printed outcome physically tests curvature transitions, layer continuity, and toolpath execution on a geometry representative of the proposed habitat shell. Because fabrication follows the same path-planning logic as the intended construction workflow, the scaled print provides empirical evidence that multi-directional curvature can be produced without the trajectory constraints typical of gantry-based systems, especially relevant for spherical, pressure-containing envelopes where uninterrupted deposition is desirable. This is an important distinction, because most Earth-based 3D construction is not only always vertical, but commonly performed using gantry-based systems, whereas robotic-arm-based printing is less common and is generally limited to single walls or relatively small objects. This supports the use of scaled robotic prints as a low-risk validation step for multi-axis path-planning before full-scale construction trials.

A key contribution of the study is the slab experiment, which targets one of the most difficult aspects of additive construction: producing horizontal elements without formwork. The close agreement between SAP2000 predictions and the measured free-end (tip) deflection indicates that the coordinate-driven workflow can produce scaled members with structural response consistent with numerical modeling. This aligns directly with the objective of integrating robotic construction logic with a Martian habitat structural concept that includes slab printing as a functional requirement. In this sense, the study also departs from current Earth-based practice, since multi-story buildings would require slabs to be printed by robotic arm, a task that is not normally performed in terrestrial 3D building printing. Under Martian gravity, which is about 38% of Earth's gravity, printing slabs in place may become more feasible, and taking advantage of this low-gravity condition constitutes another novelty of the study.

In the broader Mars construction context, this validation is particularly relevant for polymer-based structural systems, where both stiffness and strength are substantially higher than hot-glue used in this lab study. The cantilever slab demonstration reinforces this point by showing that section geometry can compensate for low material stiffness to maintain stability during and after deposition. In addition, unlike most Earth-based printed buildings that primarily employ vertical wall systems, Martian habitats must respond to a radically different environmental demand because the atmospheric pressure on Mars is only about 0.6% of that on Earth. As a result, the building envelope must resist a large pressure difference between interior and exterior conditions, and this makes the search for structural form fundamentally different from that of terrestrial 3D printed construction.

Finally, the material choice should be interpreted correctly: hot glue is suitable here as a process surrogate for studying deposition continuity, curvature fidelity, and layer bonding behavior, but it does not represent the target structural material performance. Hot glue is used as a process surrogate; therefore, the results are interpreted in terms of print controllability and constructability, not final structural strength. This aligns with the research strategy of first validating the robotic deposition workflow and then translating it to CO_2-derived polymer concepts under Mars-relevant constraints [7].

5 Conclusion

This study investigated the applicability of a six-degree-of-freedom (6-DoF) robotic arm for additive manufacturing of structural and architectural components relevant to Martian habitat construction. Using a coordinated workflow that integrates Excel-based toolpath definition (position, orientation, and speed), a Python-ROS control interface, and a custom hot-melt extrusion system, a sequence of calibration and application-level prints was conducted to assess geometric fidelity and constructability at reduced scale.

The calibration experiments established stable deposition and provided a parameter baseline for printing both planar and multi-curved geometries. Application-level demonstrations, including the flat unit, the 1/35-scale Marsphere prototype produced within the SFM logic, and the cantilever slab, show that the proposed workflow can reproduce curvature transitions, maintain continuous toolpaths, and fabricate a formwork-free horizontal element at the tested scale.

Overall, the results support scaled robotic fabrication as a practical intermediate step between digital planning and future construction scenarios. Future work will focus on multi-material extrusion, testing under low-pressure environments, and integrating in-situ resource utilization to bridge laboratory-scale studies and operational extraterrestrial construction missions.

The originality of the study lies in integrating coordinate-based toolpath generation, Python-ROS robotic execution, multi-curved shell fabrication, and formwork-free slab validation into a single experimentally demonstrated workflow for Martian habitat construction. In this sense, the study moves beyond isolated printing demonstrations and provides a practical validation framework linking digital planning, robotic fabrication, and structural relevance.

Acknowledgements

This work was supported by METU Office of Scientific Research Projects Coordination (BAP), and the authors gratefully acknowledge their financial support. The authors also gratefully acknowledge TÜBİTAK for supporting conference participation.

References

[1] R. P. Mueller, T. J. Prater, M. Roman, J. E. Edmunson, M. R. Fiske, and P. Carrato. NASA Centennial Challenge: Three Dimensional (3D) Printed Habitat, Phase 3. In *Proceedings of the 70th International Astronautical Congress (IAC)*, paper IAC-19-E5.1.8, Washington, D.C., USA, 2019.

[2] S. O. Starr and A. C. Muscatello. Mars in situ resource utilization: a review. *Planetary and Space Science*, 182:104824, 2020.

[3] I. Ishak and P. Larochelle. Robot Arm Platform for Additive Manufacturing: 3D Lattice Structures. In *Proceedings of the 30th Florida Conference on Recent Advances in Robotics (FCRAR)*, Florida Atlantic University, Boca Raton, FL, USA, 11–12 May 2017; pp. 1–5.

[4] Y. Zhi, T. Teng, and M. Akbarzadeh. Designing 3D-printed concrete structures with scaled fabrication models. Architectural Intelligence, 3:28, 2024. https://doi.org/10.1007/s44223-024-00070-3

[5] M. Quigley, B. Gerkey, K. Conley, J. Faust, T. Foote, J. Leibs, E. Berger, R. Wheeler, and A. Y. Ng. ROS: an open-source Robot Operating System. In *Proceedings of the ICRA Workshop on Open Source Software*, Kobe, Japan, 2009.

[6] Universal Robots. UR5e e-Series datasheet. Online: https://www.universal-robots.com/media/1807465/ur5e_e-series_datasheets_web.pdf, Accessed: 07/01/2026.

[7] E. Koca and A. Türer. Design, Optimization, and Autonomous Construction of Martian Infrastructure Including Slabs Using In-situ CO_2-Based Polyethylene. Journal of Building Engineering, 98:111318, 2024.